analytical chemistry

Article

Cite This: Anal. Chem. 2019, 91, 11178−11184

pubs.acs.org/ac

Calibration-Free Nanopore Digital Counting of Single Molecules

Reza Nouri,[†] Zifan Tang,[†] and Weihua Guan*[,†,‡]

[†]Department of Electrical Engineering, Pennsylvania State University, University Park, Pennsylvania 16802, United States

[‡]Department of Biomedical Engineering, Pennsylvania State University, University Park, Pennsylvania 16802, United States

Supporting Information

ABSTRACT: Nanopore sensor conceptually represents an ideal single molecule counting device due to its unique partitioning-free, label-free electronic sensing. Existing theories and experiments have shown that sample concentration is proportional to the molecule translocation rate. However, a detailed nanopore geometry and size characterization or a calibration curve of concentration standards are often required for quantifying the unknown sample. In this work, we proposed and validated a calibration-free nanopore single molecule digital counting method for isolated molecule quantification. With the background ions as the in situ references, the molecule translocation rates can be normalized to the ion translocation rates (i.e., baseline current). This in situ reference alleviates the requirement for knowing the nanopore geometry and size or generating a calibration curve. In recognition of this effect, we developed a quantitative model for nanopore quantification without the need for prior knowledge of experimental conditions such as nanopore geometry, size, and applied voltage. This model was experimentally validated for different nanopores and DNA molecules with different sizes. We anticipate this calibration-free digital counting approach would provide a new avenue for nanopore-based molecule sensing.

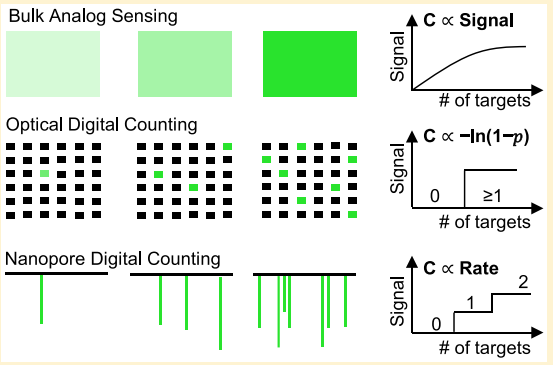

Quantification of isolated biomolecules such as DNAs, RNAs, and proteins is of critical importance for various applications in environmental, medical, and food science studies.[1,2] This process is routinely accomplished by bulk-based optical sensing methods such as UV−Vis spectrophotometry[3] or dye-based fluorimetry.[4] The resulting analog readout signal is proportional to the bulk sample concentration, the value of which can be determined with a reference curve (Figure 1a). In contrast to the analog sensing method, digital assays have emerged as a highly sensitive approach for concentration quantification.[5] Notable examples include digital PCR,[6−8] digital ELISA (enzyme-linked immunosorbent assay),[9−11] and digital ELOHA (enzyme-linked oligonucleotide hybridization assay).[12] The general concept of the digital assays is that the sample is physically partitioned into many small chambers such that each partition contains a discrete number of molecules (0, 1, 2, . . .). Each partition gives a binary 0 or 1 signal corresponding to the case of no molecule presented and at least one molecule presented, respectively. Note that the digital assay does not necessarily mean each partition has either zero or one molecule. With Poisson statistics, the sample concentration can be estimated by $-\ln(1-p)$, where p is the ratio of the positive partitions over total partitions (Figure 1b).

The digital assays so far are predominated by physical partitioning and optical detection methods to generate the binary signal. Nanopore-based sensors[13−27] allow single molecules to be analyzed electronically without the need for labeling and partitioning. Conceptually, nanopore sensor represents an ideal single molecule counting device due to its unique features of label-free electronic sensing, single-molecule sensitivity, and potential reusability. When a single molecule is electrophoretically driven through the nanopore, a detectable ionic current blockade generates a digital "1" signal, the rate of which is proportional to the sample concentration (Figure 1c). Resolving this digital event itself is much easier than analyzing its analog features such as magnitude and duration of the current dip.

Existing theories[16,28,29] and experiments[13,30,31] have shown that when interactions between molecules are negligible, the molecule molar concentration (mol/m^3) is linearly related to the translocation rate (s^{-1}) as $R = \alpha N_A C$, where N_A is the Avogadro constant and α is usually referred to as the capture rate.[28,32] Wanunu et al. successfully applied this principle to quantify the isolated miR122a electronically.[33] Since capture rate α strongly depends on experimental parameters such as nanopore geometry,[28,34] temperature,[30,35] molecule size,[16] and applied voltage,[36,37] a calibration curve of the rate versus concentration was necessary to infer the unknown sample concentration.[33] Moreover, the calibration curve must be obtained under the same experimental conditions for comparable capture rate α. Unfortunately, generating this calibration curve is often time-consuming and challenging due to nanopore clogging issues.[38,39]

Received: April 20, 2019
Accepted: July 12, 2019
Published: July 19, 2019

DOI: 10.1021/acs.analchem.9b01924
Anal. Chem. 2019, 91, 11178−11184

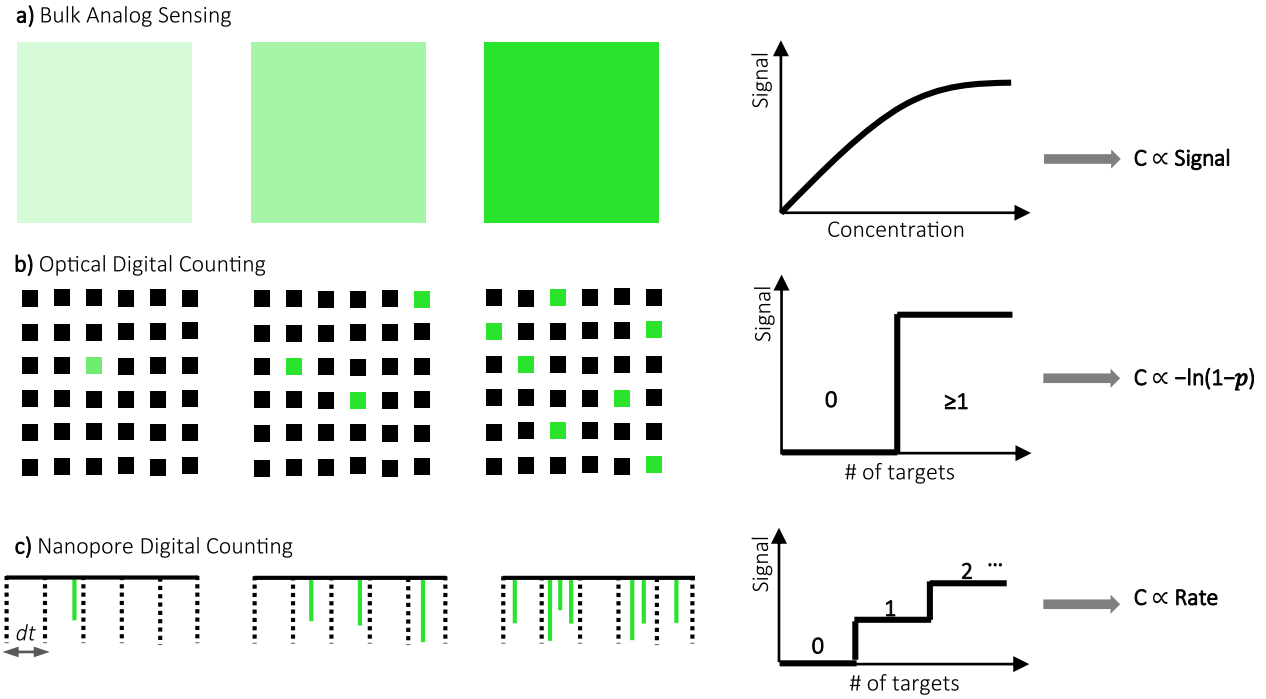

Figure 1. Comparisons for different quantification methods. (a) Analog sensing generates a signal proportional to the bulk sample concentration. (b) In the optical digital counting, the sample is partitioned into many small containers such that each partition contains a discrete number of biological entities. The sample concentration is determined by Poisson statistics (p is the positive ratios). (c) In nanopore digital counting, the sample concentration is proportional to the single molecule translocation rates.

In this work, we set out to develop a calibration-free nanopore single molecule counting method for isolated molecule quantification. We first studied the statistics of the molecule translocation rate and developed an experimentally practical method to measure the rate. We developed a quantitative model for molecule quantification without the need for prior knowledge of experimental conditions such as nanopore geometry, size, and applied voltage. This is achieved by using the background ions as the in situ reference such that the molecule translocation rates can be normalized to the ion translocation rates (baseline current). This model was experimentally validated for different nanopores and DNA molecules with different sizes. While the results presented in this work were from glass nanopores and DNA molecules, the principle could be well extended to other nanopore types and other charged molecules.

EXPERIMENTAL SECTION

Materials and Chemicals. 0.2 mm Ag wires (Warner Instruments, Hamden, USA) were used to fabricate the Ag/AgCl electrodes in house. Microinjectors of 34 gauge was purchased from World Precision Instruments. Potassium chloride and Tris-EDTA-buffer solution (10 mM Tris-HCl and 1 mM EDTA) were purchased from Sigma-Aldrich. Piranha solution was made by mixing concentrated sulfuric acid (H_2SO_4) with hydrogen peroxide (H_2O_2). Quartz capillaries with inner and outer diameter of 0.5 mm and 1 mm were purchased from Sutter Instrument. We filtered the testing solutions with a 0.2 μm syringe filter (Whatman). DNA templates (λ-DNA, 10 kbp, and 5 kbp DNA with the concentration of 0.5 μg/μL) were purchased from ThermoFisher.

Glass Nanopore Fabrication. The quartz capillaries were first cleaned in Piranha solution for 30 min to remove organic residues, then rinsed with DI water, and dried in an oven at 120 °C for 15 min. A two-line recipe, (1) heat 750, filament 5, velocity 50, delay 140, and pull 50; (2) heat 710, filament 4, velocity 30, delay 155, and pull 215, were used to pull the capillaries with a laser pipet puller (P-2000, Sutter Instruments, USA). This recipe typically produces nanopore size around 10 nm. Despite known batch-to-batch variations in size, the method presented in this work is valid as long as the nanopore can resolve the single molecule translocation (rather than multiple molecules).

Glass Nanopore Characterization with I–V, SEM, and TEM. Glass nanopore characterization was performed by standard I–V measurement, SEM, and TEM imaging. For I–V characterization, the glass nanopore was filled with 1 M KCl in Tris-EDTA buffer by a microinjector and then immersed in the testing solution. Home-made Ag/AgCl electrodes were used for interfacing the electrical measurement (Figure 2a), and the I–V curve was recorded for nanopore size estimation (Figure 2b). For SEM imaging (Figure 2c), the glass nanopore was coated with 5 nm thick of iridium to avoid the charging effect. TEM characterization was also performed to obtain detailed information for the nanopore geometry and size (Figure 2d).

Single Molecule Counting Measurement and Data Analysis. The schematic of the single molecule counting setup is illustrated in Figure 2a. One molar KCl in Tris-EDTA buffer was used for all DNA experiments to decrease the effect of electroosmotic flow.[40] A voltage was applied across the nanopore by a 6363 DAQ card (National Instruments, USA). The resulting current was amplified by a transimpedance amplifier (DLPCA-200, FEMTO, Germany) and then digitalized by 6363 DAQ card with a 100 kHz sampling rate. The recorded current time trace was analyzed by a customized MATLAB (MathWorks) software to extract the single molecule translocation information regarding the interarrival

DOI: 10.1021/acs.analchem.9b01924
Anal. Chem. 2019, 91, 11178−11184

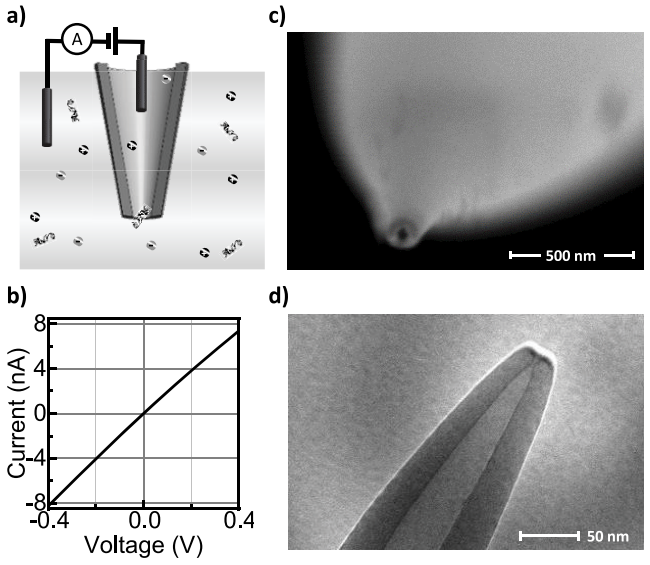

Figure 2. Experimental setup and nanopore characterization. (a) Illustration of the experimental setup (not to scale). Ag/AgCl electrodes were inserted to the nanopore and bulk solution to apply the bias voltage across the nanopore. (b) A typical IV curve for glass nanopore in 1 M KCl with Tris-EDTA-buffer solution. (c) SEM image of the glass nanopore showing the overall shape. (d) The TEM image of the nanopore tip showing apparent conical shape.

time between translocation events, the ionic current dip, and the molecule dwell time.

RESULTS AND DISCUSSION

It was previously observed that the mean time between single-molecule capture events in solid-state nanopore follows an exponential distribution,[34] indicating a Poisson process.[34,41] To validate if this is also true in our glass nanopore, we performed studies on λ-DNAs with a serial of concentrations ranging from 12 to 60 pM. A quick eyeball on the current time traces in Figure 3a shows that translocation occurs more often as the concentration increases. The extracted interarrival time distribution also shows a remarkable exponential distribution for each concentration (Figure 3b). Note that the exponential fits to these distributions are usually used to obtain the hidden translocation rate.[16,34] To further confirm the Poisson process, the same raw data sets were used to extract the probability distribution $P(n)$ for observing n events within a fixed time interval (Figure 3c). Each concentration case is then fitted with a Poisson distribution, $P(n) = e^{-\lambda}\lambda^n/n!$, where λ is the expected occurrence of the events. In a process with the rate of R, $\lambda = Rdt$ where dt is the time interval.[34] As shown in Figure 3d, both fittings to the exponentially distributed interarrival time and fittings to the Poisson distribution yield comparable rate determination at different concentrations. Figure 3d also shows there is a linear relationship between translocation rate and the

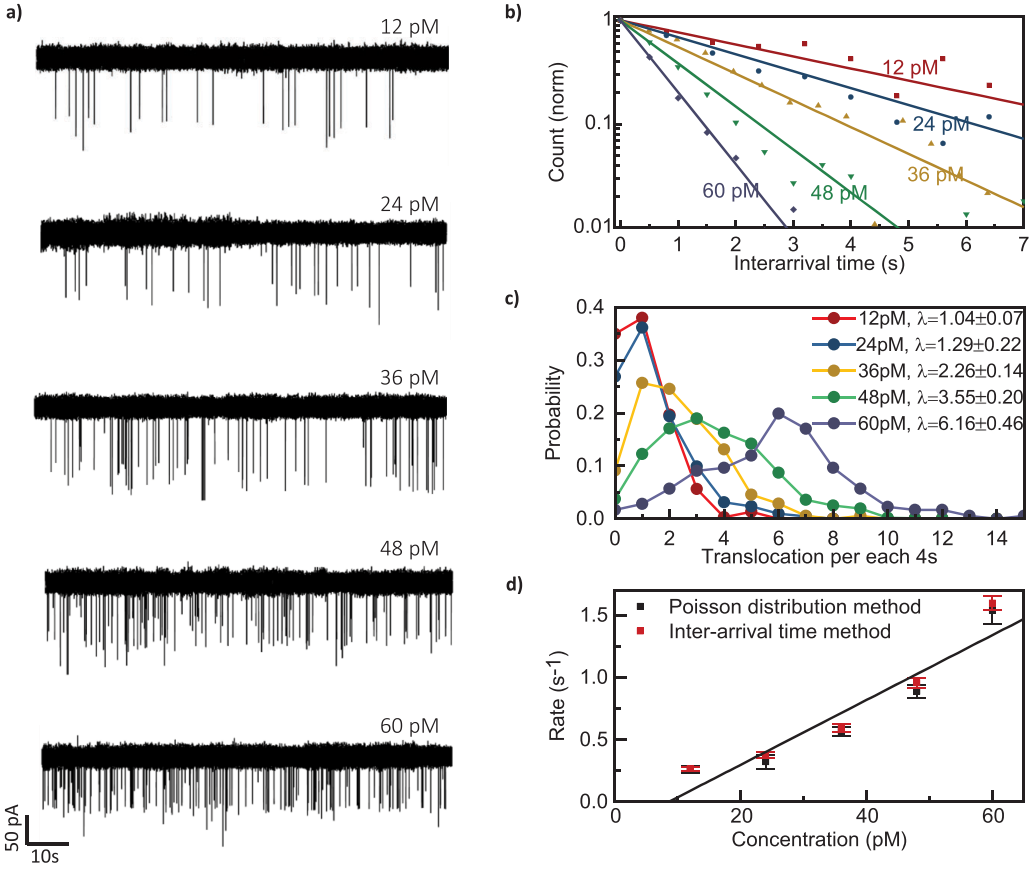

Figure 3. Translocation recording of λ-DNA through glass nanopore at 1 M KCl under 400 mV bias. (a) Continuous current readout illustrating the translocation events at different DNA concentrations. The average molecular distance is around 3 μm, the interactions between molecules are negligible. (b) Normalized distributions of interarrival time for different concentrations with monoexponential fits to the distributions. (c) The probability distribution of the events for different concentrations. The 4 s time interval is used to better show the Poisson distribution. (d) The translocation rate obtained from both fitting methods versus the λ-DNA concentrations.

DOI: 10.1021/acs.analchem.9b01924
Anal. Chem. 2019, 91, 11178−11184

DNA concentrations in the glass nanopores, consistent with the theory prediction[28] and previous experimental studies.[13,29,30]

While both fitting methods provide a measure of the rate R, the result can only be obtained off-line after enough digital events were registered to generate sufficient data points for fitting. A more practical approach to determine the rate online is by counting the number of events per certain time while the experiment is ongoing. Since the translocation events follow the Poisson process, assuming n discrete single-molecule translocation events were observed in a particular observation time window T, one can infer the rate with a certain confidence interval as $(n \pm z(n)^{1/2})/T$, where z is the standard score. The 95% confidence interval of the rate is $(n \pm 1.96(n)^{1/2})/T$.[42] We denote this approach as the n/T method hereafter. The relative uncertainty of inferring the rate R is proportional to $n^{-1/2}$. It is thus clear that there is a trade-off between minimizing the uncertainty (increasing n) and achieving real-time rate determination (reducing n). Figure 4 compares the inferred rate using the online n/T method to the rate determined by the Poisson fitting method, using 12 pM λ-DNA sample. Two features were observed when more digital translation events were observed. First, the relative uncertainty (error bars) was reduced to that of the Poisson fitting method. Second, the mean rate estimation (diamonds) converged to the translocation rate obtained from the Poisson fitting method. These two features can be seen quantitively in the inset of Figure 4, i.e., as more digital translations were observed, both mean and uncertainty ratios converge to 1. This validates the n/T method for rate determination as long as sufficient translocations were observed. Experimentally, we examined at least 200 events for a measurement uncertainty < 7%.

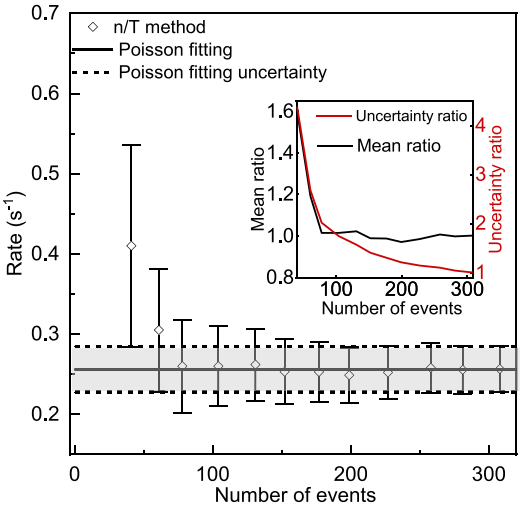

Figure 4. Translocation rate determined by the n/T method for increasing the observation numbers. The shaded area is the value obtained by the Poisson fitting method (mean + uncertainty). The inset shows the mean and uncertainty value comparison between these two methods.

With an experimentally efficient n/T approach to determine the rate, the next task is to determine the capture rate α. The dynamics of molecule translocation through the nanopore consists of three steps: (1) the molecule moves from the bulk of the reaction chamber toward the pore entrance by a combination of diffusion and drift forces; (2) the molecule is captured at the entrance of the nanopore; and (3) the molecule overcomes an entropy energy barrier and goes through the nanopore, causing a detectable ionic current blockade which can be detected electronically as a digital signal.[28] It is known that the capture rate α could be diffusion limited (step 1) or barrier limited (step 3).[16] The glass nanopores used in our experiments are around 10 nm in size, which is large enough such that the transport is diffusion limited rather than barrier limited,[43,44] as indicated by the linear dependence of the capture rate on the voltage (Figure S1).

In the diffusion-limited region, the capture rate for the conical-shaped glass nanopore is given by $\alpha = 2\pi\mu\tilde{d}\,\Delta V$, where μ is the free solution electrophoretic mobility, ΔV is the applied electric potential across the pore, and $\tilde{d}$ is the characteristic length of the nanopore (see the Supporting Information). If the nanopore geometry and size is explicitly known for a particular experiment, the capture rate can be directly calculated to determine the unknown sample concentration without calibration, similar to a pressure-driven calibration-less quantitation of nanoparticles by calculating the hydrodynamic resistance.[45] Nevertheless, it is well-known that glass nanopore geometry is widely dispersed.[46] TEM characterization of each nanopore is often destructive and is time-, facility-, and expertise-intensive.[47] In addition, experimental conditions such as applied voltage, temperatures, and buffers also vary from one experiment to the other. To properly determine the unknown sample concentration, a calibration curve must be obtained under the same experimental conditions to extract the capture rate α in that particular experiment.[16] While this could be done, it is often time-consuming and experimentally challenging due to potential nanopore clogging under repetitive testing.[38]

To overcome these challenges, we here developed an in situ method for determining the capture rate α without the need for prior knowledge on nanopore experimental conditions. This is achieved by recognizing that the baseline current carries information about the background ion translocation rate (Figure 5a). Therefore, it is feasible to use the ionic concentration (generally known for a particular experiment) as the internal reference to estimate the unknown capture rate α. The baseline current can be estimated as $I_b = 2\pi\Lambda C_{ion}\tilde{d}\,\Delta V$ (Supporting Information), where Λ is the molar conductivity which depends on the mobility and valence of the ions as $\Lambda = \Sigma_i N_A e z_i \mu_i$.[48] The previously inaccessible parameter $\alpha = 2\pi\mu\tilde{d}\,\Delta V$ can be rewritten as

$$\alpha = \frac{\mu I_b}{\Lambda C_{ion}} \tag{1}$$

Eq 1 implies that the unknown capture rate can be derived from the experimentally accessible baseline current and the ionic concentration without knowing the nanopore geometry, size, and the applied voltage. The molecule mobility μ and molar conductivity Λ can be estimated for a particular molecule and salt. Thus, the molecule translocation rate $R = \alpha N_A C_{mol}$ can be written as

$$R = \frac{\mu N_A C_{mol}}{\Lambda C_{ion}} I_b \tag{2}$$

DOI: 10.1021/acs.analchem.9b01924
Anal. Chem. 2019, 91, 11178−11184

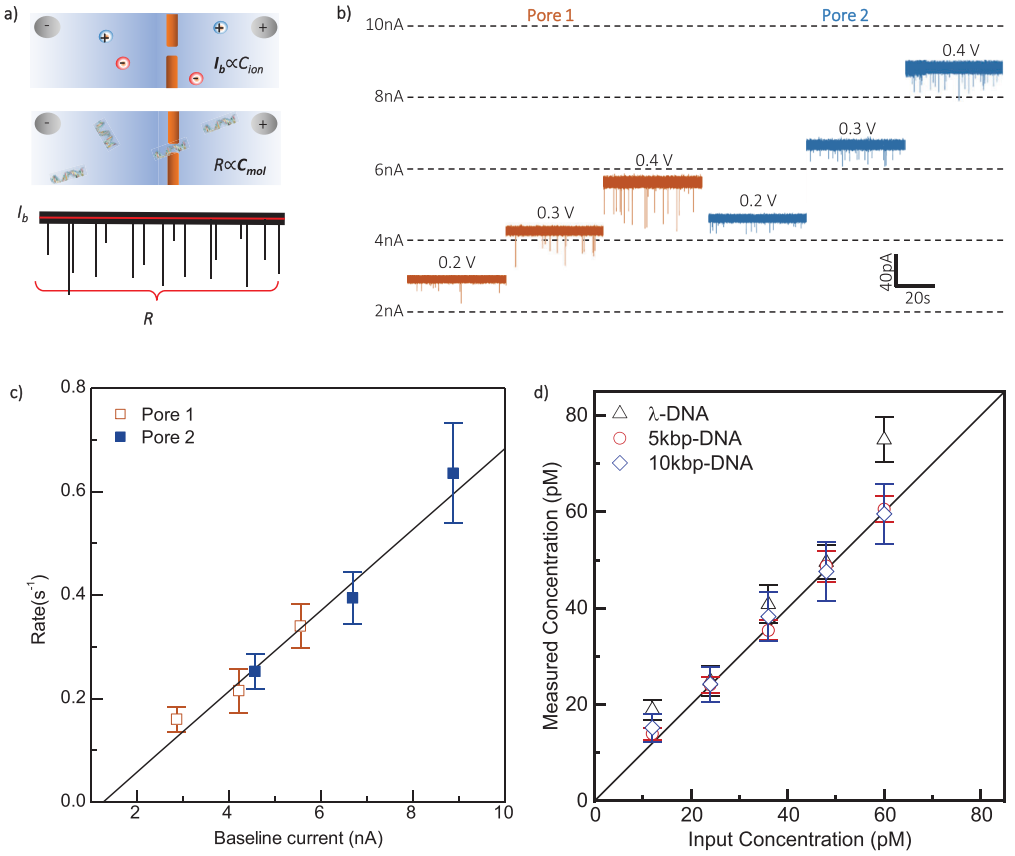

Figure 5. (a) Schematic of ions and molecules translocation through the same nanopore. The ion and molecule translocation rate is experimentally obtainable from the continuous current readout. (b) Current time trace of 24 pM 10 kbp DNA (in 1 M KCl) translocating through two different nanopores under different voltages. (c) The molecule translocation rate is linearly proportional to the baseline current for the same test sample shown in (b). (d) Validation of the calibration-free method for concentration determination. The test was performed with different nanopores and DNA molecules with different sizes.

Table 1. Summary of Calibration-Free Method for Quantifying Concentration

sample	input concentration (pM)	I_b (nA)	R (1/s)	measured concentration (pM)[a]	error (%)[b]
λ-DNA	12	6.06	0.26 ± 0.03	18.90 ± 2.07	57.50
	24	5.93	0.34 ± 0.05	24.90 ± 3.11	3.75
	36	6.28	0.58 ± 0.04	40.78 ± 3.92	13.29
	48	8.19	0.92 ± 0.05	49.54 ± 3.54	3.20
	60	8.40	1.43 ± 0.11	74.93 ± 4.65	24.88
5 Kbps DNA	12	3.96	0.13 ± 0.01	13.89 ± 1.27	15.74
	24	4.03	0.22 ± 0.01	24.11 ± 1.64	0.45
	36	4.05	0.33 ± 0.02	35.36 ± 2.07	−1.77
	48	4.03	0.45 ± 0.03	48.70 ± 3.24	1.46
	60	4.46	0.61 ± 0.03	60.49 ± 2.71	0.82
10 Kbps DNA	12	6.21	0.21 ± 0.04	15.15 ± 2.87	26.30
	24	6.21	0.34 ± 0.05	24.22 ± 3.63	0.93
	36	6.27	0.54 ± 0.07	38.23 ± 5.07	6.19
	48	6.83	0.74 ± 0.09	47.59 ± 6.08	−0.85
	60	8.51	1.15 ± 0.12	59.53 ± 6.24	−0.78

[a]Calculated using eq 3 with parameters: $\mu = 4.1 \times 10^{-8}$ m^2 V^{-1} s^{-1}, $\Lambda = 10.86$ m^{-1} M^{-1} S, $C_{ion} = 1$ M. [b]Error is defined as (measured − input)/input ×100%.

To validate eq 2, we performed experiments with 10 kbp DNA at 24 pM in the 1 M KCl buffer solution. Figure 5b shows the current time trace at different applied voltages for two glass nanopores pulled from different batches. Two features can be observed. First, higher applied voltage leads to a higher molecule translocation rate, consistent with previous reports.[16] Second, due to the nanopore size variation, the same applied voltage does not generate the same molecule translocation rate. This dependence of the translocation rate on applied voltages and the nanopore sizes indicates that a calibration curve must be obtained under the same experimental conditions (the same pore and applied voltage).[31] Fortunately, eq 2 predicts that the molecule translocation rate scales linearly with the baseline current for

DOI: 10.1021/acs.analchem.9b01924
Anal. Chem. 2019, 91, 11178−11184

a fixed testing molecule and salt concentrations. This is exactly what we observed in Figure 5c. The molecule translocation rate versus the I_b indeed falls into a single line for different pores at different applied voltages.

After verifying this in situ ionic current reference model, calibration-free quantification of the molecule molar concentration can thus be performed by rewriting eq 2 as

$$C_{mol} = \frac{\Lambda R}{\mu N_A I_b} C_{ion} \quad (3)$$

Eq 3 shows that unknown sample concentration can be quantified without explicitly knowing the nanopore geometry, size, and the applied voltage, as long as the parameters on the right-hand side of the equation could be determined. To validate this method, we tested λ-DNA, 5 kbp DNA, and 10 kbp DNA at five known concentrations (12, 24, 36, 48, and 60 pM) in 1 M KCl buffer, intentionally using glass nanopores pulled from different batches. Since the free solution electrophoretic mobility of DNA in the Tris-EDTA buffer was theoretically[49] and experimentally[50] shown to be independent of the DNA length longer than a few persistence lengths,[51] μ of 4.5×10^{-8} m^2 V^{-1} s^{-1} was used for all DNA molecules.[52] The buffer solution is dominated by 1 M KCl, and thus the molar conductivity Λ is estimated to be 10.86 m^{-1} M^{-1} S.[48] Table 1 summarizes the results for this calibration-free method for concentration measurement. The baseline current (I_b) and translocation rate (R) was determined from the experiment. Figure 5d plots the measured versus the input concentration for all tests. All data points falling into a straight line of slope 1, indicating the accuracy of the calibration-free method. It is noteworthy that the molecule concentration determined by eq 3 is widely applicable to other kinds of molecules as long as their electrophoretic mobility was known.

One important aspect of the nanopore single molecule counting method is the upper and lower bound for concentrations (dynamic range). The upper bound is related to the maximum count rate, which is determined by the speed of the electronic detector and the jamming effect when too many molecules are translocating at the same time.[35] On the other hand, the lower bound (limit of detection) is determined by two factors. The first is the false positive rate when no molecule exists in the testing sample. This is similar to the dark count rate in the single photon counters.[53] This false positive rate determines the minimum count rate at which the signal is dominantly caused by real molecules presented. The false detection events are mostly due to the noise in the testing apparatus. The second factor is the uncertainty in the Poisson rate determination (Figure 4). Since relative uncertainty of inferring the rate R is proportional to $n^{-1/2}$, a large enough event numbers (N) should be recorded to establish a sufficiently robust statistical basis. With the translocation rate R, a minimal recording time of N/R is thus required. Assuming a practical measurement time of T, a minimal translocation rate N/T is required, which corresponds to the lower bound of the molecule concentration. For example, if we need N to be 200 events and a practical experiment time of 30 min, the minimum rate should be around 0.1/s, corresponding to ~10 pM in our experimental setup.

CONCLUSION

In summary, we presented a nanopore single molecule digital counting method for isolated molecule quantification without the need for prior knowledge of experimental conditions such as nanopore geometry, size, and applied voltage. When single molecules were electrophoretically driven through the 10 nm glass nanopore one by one, digital events were registered. We observed that these digital translocation events follow the Poisson distribution, consistent with other types of nanopores.[34] We developed a Poisson statistics-based approach to determine the rate with a certain confidence interval while the experiment is ongoing. We recognized that the ionic rates (baseline current) in a particular experiment could be used as an effective in situ reference. We developed a quantitative model for calibration-free quantification of molecule concentration, which was experimentally validated for different nanopores and DNA molecules. It is noteworthy that the method is currently validated in high salt concentration. At low salt concentrations, the electroosmotic flow would start affecting the translocation dynamics,[40] and we are performing a systematic study to understand the dynamics in this region. While the results presented in this work were from glass nanopores and DNA molecules, the principle could be well extended to other nanopore types and other charged molecules. We anticipate this calibration-free digital counting approach would provide a new avenue for nanopore sensors.

ASSOCIATED CONTENT

Supporting Information

The Supporting Information is available free of charge on the ACS Publications website at DOI: 10.1021/acs.analchem.9b01924.

Derivation of capture rate for conical shape nanopore; baseline ionic current derivation; and translocation rate and applied voltage relationship (PDF)

AUTHOR INFORMATION

Corresponding Author

*E-mail: w.guan@psu.edu. Tel: 1-814-867-5748.

ORCID

Weihua Guan: 0000-0002-8435-9672

Author Contributions

W.G. conceived the concept and supervised the study, R.N. and Z.T. designed and performed the nanopore experiments, R.N. and W.G. analyzed the data, and all authors cowrote the manuscript.

Notes

The authors declare no competing financial interest.

ACKNOWLEDGMENTS

This work supported by the National Science Foundation under Grant 1710831. Any opinions, findings, and conclusions or recommendations expressed in this work are those of the authors and do not necessarily reflect the views of the National Science Foundation. W.G. acknowledges the support from Penn State Startup Fund.

REFERENCES

(1) Cretich, M.; Daaboul, G. G.; Sola, L.; Ünlü, M. S.; Chiari, M. *Trends Biotechnol.* **2015**, *33*, 343−351.

(2) Calderón-Celis, F.; Sugiyama, N.; Yamanaka, M.; Sakai, T.; Diez-Fernández, S.; Calvete, J. J.; Sanz-Medel, A.; Encinar, J. R. *Anal. Chem.* **2019**, *91*, 1105−1112.

(3) Haiss, W.; Thanh, N. T.; Aveyard, J.; Fernig, D. G. *Anal. Chem.* **2007**, *79*, 4215−4221.

DOI: 10.1021/acs.analchem.9b01924
Anal. Chem. 2019, 91, 11178−11184

(4) Niesen, F. H.; Berglund, H.; Vedadi, M. *Nat. Protoc.* **2007**, *2*, 2212.
(5) Basu, A. S. *SLAS TECHNOLOGY: Translating Life Sciences Innovation* **2017**, *22*, 369−386.
(6) Vogelstein, B.; Kinzler, K. W. *Proc. Natl. Acad. Sci. U. S. A.* **1999**, *96*, 9236−9241.
(7) Hindson, C. M.; Chevillet, J. R.; Briggs, H. A.; Gallichotte, E. N.; Ruf, I. K.; Hindson, B. J.; Vessella, R. L.; Tewari, M. *Nat. Methods* **2013**, *10*, 1003.
(8) Hindson, B. J.; Ness, K. D.; Masquelier, D. A.; Belgrader, P.; Heredia, N. J.; Makarewicz, A. J.; Bright, I. J.; Lucero, M. Y.; Hiddessen, A. L.; Legler, T. C. *Analytical chemistry* **2011**, *83*, 8604−8610.
(9) Rissin, D. M.; Kan, C. W.; Campbell, T. G.; Howes, S. C.; Fournier, D. R.; Song, L.; Piech, T.; Patel, P. P.; Chang, L.; Rivnak, A. J.; et al. *Nature biotechnology* **2010**, *28*, 595.
(10) Leirs, K.; Tewari Kumar, P.; Decrop, D.; Pérez-Ruiz, E.; Leblebici, P.; Van Kelst, B.; Compernolle, G.; Meeuws, H.; Van Wesenbeeck, L.; Lagatie, O.; et al. *Analytical chemistry* **2016**, *88*, 8450−8458.
(11) Cohen, L.; Walt, D. R. *Annu. Rev. Anal. Chem.* **2017**, *10*, 345−363.
(12) Guan, W. H.; Chen, L. B.; Rane, T. D.; Wang, T. H. *Sci. Rep-Uk* **2015**, *5*, 13795.
(13) Bell, N. A.; Muthukumar, M.; Keyser, U. F. *Phys. Rev. E: Stat. Phys., Plasmas, Fluids, Relat. Interdiscip. Top.* **2016**, *93*, 022401.
(14) Rowghanian, P.; Grosberg, A. Y. *Phys. Rev. E* **2013**, *87*, 042722.
(15) Nomidis, S. K.; Hooyberghs, J.; Maglia, G.; Carlon, E. *J. Phys.: Condens. Matter* **2018**, *30*, 304001.
(16) Wanunu, M.; Morrison, W.; Rabin, Y.; Grosberg, A. Y.; Meller, A. *Nat. Nanotechnol.* **2010**, *5*, 160.
(17) McNally, B.; Wanunu, M.; Meller, A. *Nano Lett.* **2008**, *8*, 3418−3422.
(18) Venkatesan, B. M.; Bashir, R. *Nat. Nanotechnol.* **2011**, *6*, 615.
(19) Liu, K.; Pan, C.; Kuhn, A.; Nievergelt, A. P.; Fantner, G. E.; Milenkovic, O.; Radenovic, A. *Nat. Commun.* **2019**, *10*, 3.
(20) Varongchayakul, N.; Hersey, J. S.; Squires, A.; Meller, A.; Grinstaff, M. W. *Adv. Funct. Mater.* **2018**, *28*, 1804182.
(21) Plesa, C.; Verschueren, D.; Pud, S.; van der Torre, J.; Ruitenberg, J. W.; Witteveen, M. J.; Jonsson, M. P.; Grosberg, A. Y.; Rabin, Y.; Dekker, C. *Nat. Nanotechnol.* **2016**, *11*, 1093.
(22) Freedman, K. J.; Otto, L. M.; Ivanov, A. P.; Barik, A.; Oh, S.-H.; Edel, J. B. *Nat. Commun.* **2016**, *7*, 10217.
(23) Piguet, F.; Ouldali, H.; Pastoriza-Gallego, M.; Manivet, P.; Pelta, J.; Oukhaled, A. *Nat. Commun.* **2018**, *9*, 966.
(24) Harrington, L.; Alexander, L. T.; Knapp, S.; Bayley, H. *ACS Nano* **2019**, *13*, 633−641.
(25) Long, Z.; Zhan, S.; Gao, P.; Wang, Y.; Lou, X.; Xia, F. *Anal. Chem.* **2018**, *90*, 577−588.
(26) Xu, X.; Hou, R.; Gao, P.; Miao, M.; Lou, X.; Liu, B.; Xia, F. *Anal. Chem.* **2016**, *88*, 2386−2391.
(27) Roshan, K. A.; Tang, Z.; Guan, W. *Nanotechnology* **2019**, *30*, 095502.
(28) Grosberg, A. Y.; Rabin, Y. *J. Chem. Phys.* **2010**, *133*, 165102.
(29) Albrecht, T. *Annual Review of Analytical Chemistry* **2019**, *12*, 371.
(30) Wanunu, M.; Sutin, J.; McNally, B.; Chow, A.; Meller, A. *Biophys. J.* **2008**, *95*, 4716−4725.
(31) Gu, L.-Q.; Wanunu, M.; Wang, M. X.; McReynolds, L.; Wang, Y. *Expert Rev. Mol. Diagn.* **2012**, *12*, 573−584.
(32) Freedman, K. J.; Haq, S. R.; Fletcher, M. R.; Foley, J. P.; Jemth, P.; Edel, J. B.; Kim, M. J. *ACS Nano* **2014**, *8*, 12238−12249.
(33) Wanunu, M.; Dadosh, T.; Ray, V.; Jin, J.; McReynolds, L.; Drndić, M. *Nat. Nanotechnol.* **2010**, *5*, 807.
(34) Meller, A.; Branton, D. *Electrophoresis* **2002**, *23*, 2583−2591.
(35) Verschueren, D. V.; Jonsson, M. P.; Dekker, C. *Nanotechnology* **2015**, *26*, 234004.
(36) Henrickson, S. E.; Misakian, M.; Robertson, B.; Kasianowicz, J. J. *Phys. Rev. Lett.* **2000**, *85*, 3057.
(37) Fologea, D.; Uplinger, J.; Thomas, B.; McNabb, D. S.; Li, J. *Nano Lett.* **2005**, *5*, 1734−1737.
(38) Tang, Z.; Lu, B.; Zhao, Q.; Wang, J.; Luo, K.; Yu, D. *Small* **2014**, *10*, 4332−4339.
(39) Ando, G.; Hyun, C.; Li, J.; Mitsui, T. *ACS Nano* **2012**, *6*, 10090−10097.
(40) Laohakunakorn, N.; Thacker, V. V.; Muthukumar, M.; Keyser, U. F. *Nano Lett.* **2015**, *15*, 695−702.
(41) Sen, Y.-H.; Karnik, R. *Anal. Bioanal. Chem.* **2009**, *394*, 437−446.
(42) Patil, V.; Kulkarni, H. *REVSTAT-Statistical Journal* **2012**, *10*, 211−227.
(43) Chen, P.; Gu, J.; Brandin, E.; Kim, Y.-R.; Wang, Q.; Branton, D. *Nano Lett.* **2004**, *4*, 2293−2298.
(44) Gershow, M.; Golovchenko, J. A. *Nat. Nanotechnol.* **2007**, *2*, 775.
(45) Terejánszky, P.; Makra, I.; Fürjes, P. t.; Gyurcsaényi, R. b. E. *Analytical chemistry* **2014**, *86*, 4688−4697.
(46) Van den Hout, M.; Hall, A. R.; Wu, M. Y.; Zandbergen, H. W.; Dekker, C.; Dekker, N. H. *Nanotechnology* **2010**, *21*, 115304.
(47) Frament, C. M.; Dwyer, J. R. *J. Phys. Chem. C* **2012**, *116*, 23315−23321.
(48) Pratt, K. W.; Koch, W.; Wu, Y. C.; Berezansky, P. *Pure Appl. Chem.* **2001**, *73*, 1783−1793.
(49) Long, D.; Viovy, J.-L.; Ajdari, A. *Phys. Rev. Lett.* **1996**, *76*, 3858.
(50) Nkodo, A. E.; Garnier, J. M.; Tinland, B.; Ren, H.; Desruisseaux, C.; McCormick, L. C.; Drouin, G.; Slater, G. W. *Electrophoresis* **2001**, *22*, 2424−2432.
(51) Olivera, B. M.; Baine, P.; Davidson, N. *Biopolymers* **1964**, *2*, 245−257.
(52) Stellwagen, N. C.; Gelfi, C.; Righetti, P. G. *Biopolymers* **1997**, *42*, 687−703.
(53) Takeuchi, S.; Kim, J.; Yamamoto, Y.; Hogue, H. H. *Appl. Phys. Lett.* **1999**, *74*, 1063−1065.

DOI: 10.1021/acs.analchem.9b01924
Anal. Chem. 2019, 91, 11178−11184